

## ARTICLES

**Nature of band-gap states in V-doped TiO<sub>2</sub> revealed by resonant photoemission**

D. Morris, R. Dixon, F. H. Jones, Y. Dou, and R. G. Egdell\*  
*Inorganic Chemistry Laboratory, South Parks Road, Oxford OX1 3QR, United Kingdom*

S. W. Downes  
*Daresbury Laboratory, Warrington, Cheshire WA4 4AD, United Kingdom*

G. Beamson  
*Research Unit for Surfaces, Transforms and Interfaces, Daresbury Laboratory, Warrington, Cheshire WA4 4AD, United Kingdom*  
(Received 20 December 1996; revised manuscript received 3 February 1997)

Band-gap states in V-doped TiO<sub>2</sub> have been studied by photoemission spectroscopy over a range of photon energies encompassing the Ti 3*p* and V 3*p* core thresholds. The states show resonant enhancement at photon energies significantly higher than found for Ti 3*d* states introduced into TiO<sub>2</sub> by oxygen deficiency or alkali-metal adsorbates. This demonstrates that the gap states relate to electrons trapped on dopant V cations rather than host Ti cations. [S0163-1829(97)03724-7]

**I. INTRODUCTION**

The electronic properties of wide band-gap oxides such as TiO<sub>2</sub> can be strongly influenced by dopants which introduce new electronic energy levels into bulk band gaps. In the present paper we apply photoemission to study gap states associated with V doping in TiO<sub>2</sub> over a range of different exciting photon energies. It emerges that by locating resonances in the constant initial-state photoemission intensity profile it is possible to fingerprint the atomic nature of the gap states.

Investigation of the phase diagram in the V-Ti-O system by Marinder and Magneli established that TiO<sub>2</sub> and VO<sub>2</sub> exhibit an essentially continuous range of mutual solid solution and that for *x* values in Ti<sub>1-x</sub>V<sub>x</sub>O<sub>2</sub> where *x* < 0.75 the undistorted tetragonal rutile structure of TiO<sub>2</sub> itself is found.<sup>1</sup> The solid-state and surface chemistry of the V-Ti-O system has attracted widespread interest over a number of years<sup>2-5</sup> by virtue of the application of V<sub>2</sub>O<sub>5</sub> supported on TiO<sub>2</sub> as a catalyst for selective oxidation reactions.<sup>6-8</sup> For example, optimally prepared catalysts with a monolayer of V<sub>2</sub>O<sub>5</sub> on TiO<sub>2</sub> (in its anatase modification) can give up to 95% conversion of *o*-xylene to phthalic anhydride with 80% selectivity at 315 °C.<sup>8</sup> V<sub>2</sub>O<sub>5</sub> itself is widely used as a catalyst for oxidation of SO<sub>2</sub> in the contact process<sup>9</sup> and we have recently shown that V-doped TiO<sub>2</sub> also brings about catalytic oxidation of SO<sub>2</sub>, giving rise to variations in surface conductivity that can be exploited in gas sensor devices.<sup>10</sup>

Although V<sub>2</sub>O<sub>5</sub> is the thermodynamically stable vanadium oxide phase at atmospheric oxygen partial pressures up to melting point, the catalytic literature contains several measurements of weight loss from calcined V<sub>2</sub>O<sub>5</sub>/TiO<sub>2</sub> mixtures which suggest that substitutional incorporation of vanadium into the TiO<sub>2</sub> lattice facilitates reduction of V(V) to V(IV) even under atmospheric oxygen partial pressure.<sup>11,12</sup> The

weight loss measurements show that vanadium substitution is not dominantly compensated by additional defects such as cation vacancies or oxygen interstitials. This contrasts with Nb- (Ref. 13) or Ta- (Ref. 14) doped TiO<sub>2</sub>, where compensation can only be avoided at very low oxygen partial pressures. Under ambient oxygen partial pressure there is almost complete compensation by cation vacancies so that the doped material should be formulated as Ti(IV)<sub>1-5*x*/4</sub>Nb(V)<sub>*x*</sub>□<sub>*x*/4</sub>O<sub>2</sub> where the □ indicates a cation vacancy. Localized V(IV) centers in Ti<sub>1-x</sub>V<sub>x</sub>O<sub>2</sub> for low doping levels (*x* = 0.001) trap an unpaired spin to give an electron spin resonance (ESR) signal with anisotropic *g* values close to 2, characteristic of substitution into sites of the expected *D*<sub>2*h*</sub> symmetry.<sup>15-17</sup> Recent magnetic susceptibility measurements carried out in this laboratory show that in V-doped TiO<sub>2</sub> prepared by calcining V<sub>2</sub>O<sub>5</sub>-TiO<sub>2</sub> mixtures in air at 1200 °C, the unpaired spin concentration is close to the nominal V doping level.<sup>18,19</sup>

Mizushima *et al.* first attempted to locate the energy of the V 3*d* states in doped TiO<sub>2</sub>.<sup>20,21</sup> Photoconductivity and photoperturbation of the V(IV) ESR signal were monitored as a function of wavelength of doped TiO<sub>2</sub> single crystals. This allowed placement of the V 3*d* level about 2 eV below the conduction-band edge.<sup>21</sup> More recently we have carried out ultraviolet photoemission measurements on V-doped TiO<sub>2</sub> using a He discharge lamp. These measurements revealed the presence of a band-gap state at a similar energy to that found in the earlier work.<sup>18,19</sup> The band-gap state is also seen in high-resolution valence-band x-ray photoemission spectroscopy (XPS).<sup>22</sup> However, there is some ambiguity in the assignment of the photoemission gap states to electrons localized on the V dopant because at oxygen deficient TiO<sub>2-x</sub> surfaces a similar state appears in the bulk band gap.<sup>23,24</sup> This state is associated with electrons self-trapped on Ti to give a polaronic Ti 3*d*<sup>1</sup> level.<sup>25</sup>

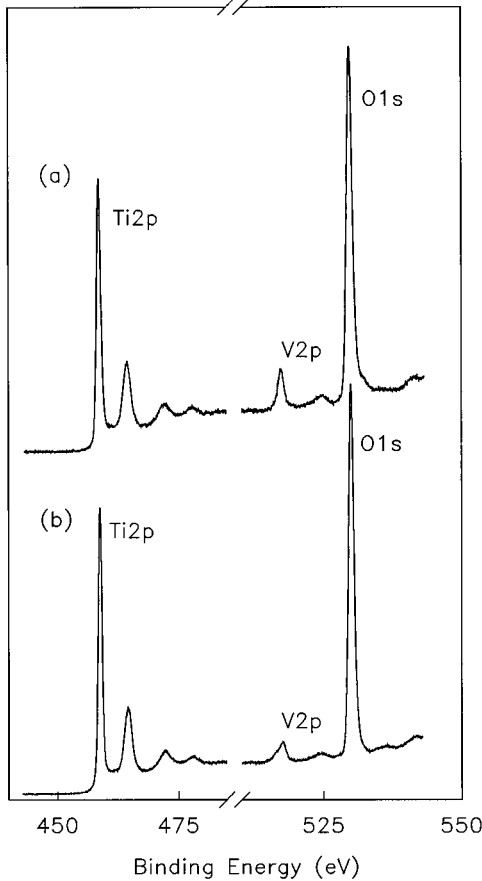


FIG. 1. Core-level XPS of 1% V-doped  $\text{TiO}_2$  taken in the Daresbury Scienta spectrometer. (a) "As-presented" sample (b) after annealing in UHV at  $620^\circ\text{C}$  for 2 h to effect sample cleaning.

It is well known that  $3d$  electron states show strong resonant enhancement at photon energies corresponding to the threshold for excitation of  $3p$  shallow core electrons.<sup>24</sup> This arises from interference between the direct photoemission channel:



and a channel where photoexcitation of a  $3p$  electron into a  $3d$  state is followed by super Coster-Kronig Auger decay to give the same final state as in direct photoemission:



The energy for resonant photoemission clearly depends on the energy of the  $3p$  core level and increases progressively on moving across the first transition series, with a shift of order 3–4 eV between successive elements such as Ti and V.<sup>26,27</sup> It is therefore to be expected that the resonance profile will provide a way of fingerprinting the electronic states in the bulk band gap of V-doped  $\text{TiO}_2$  and of distinguishing between Ti  $3d$  and V  $3d$  states.

## II. EXPERIMENT

Ceramic pellets of 1% V-doped  $\text{TiO}_2$  were prepared by intimately mixing  $\text{TiO}_2$  (Aldrich, 99.99%) and  $\text{V}_2\text{O}_5$  (Johnson Matthey, Specpure) in a water-based slurry in an agate mortar and pestle and allowing the slurry to dry at  $80^\circ\text{C}$ . The mixed powders were pressed into pellets between 13-mm tungsten carbide dies at 10 tonnes and fired at  $1200^\circ\text{C}$  in a recrystallized alumina boat for several days with intermediate regrinding and repelletization. The resulting black material gave x-ray powder diffraction profiles containing only peaks associated with a well-crystallized rutile phase: reflections due to the  $\text{V}_2\text{O}_5$  phase were completely absent. Observation of Ti  $K\alpha$  and V  $K\alpha$  emission lines in an analytical electron microscope (JEOL 2000 FX, operating at 200 keV) confirmed that the V was distributed homogeneously within the bulk of the crystallites and that no V-rich amorphous phases occurred within the samples. Following dissolution of the sample in molten sodium carbonate the absolute V doping level was determined to be 0.8%, presumably due to loss of  $\text{V}_2\text{O}_5$  during sample preparation. For convenience we refer to the nominal doping level in the subsequent discussion.

Photoemission measurements were carried out on beam-line 6.2 of the synchrotron radiation source at the Daresbury Laboratory. This incorporates a monochromator with two sets of toroidal gratings covering the photon energy ranges 15–40 eV (710 lines/mm) and 40–140 eV (1800 lines/mm). The energy analyzer has  $150^\circ$  spherical sector deflection elements of mean radius 50 mm. Energy distribution curves (EDCs) were acquired at 10-eV pass energy with 1-mm slits and  $3.3^\circ$  entrance half angle. The photon bandwidth was set at 0.1 eV. The overall experimental resolution under these conditions is about 0.15-eV full width at half maximum (FWHM). Constant initial-state spectra (CIS) were measured by scanning the analyzer synchronously with the monochromator to keep fixed on a constant initial state. For these scans the photon bandwidth was degraded to 0.2 eV and the pass energy was increased to 20 eV. Count rates were normalized relative to the drain current from a tungsten mesh beam monitor through which the synchrotron beam passed just prior to hitting the sample. To construct constant initial-state spectra curves the raw data were further corrected for the quantum efficiency of the beam monitor mesh, which had in turn been calibrated by measuring the drain current from a copper foil in the photoemission chamber.<sup>28,29</sup> All spectra were measured under normal emission with radiation incident at  $45^\circ$  to the sample surface.

Procedures for cleaning the ceramic pellets were developed in house in an ESCALAB x-ray photoelectron spectrometer equipped with an UV discharge lamp, as described in detail elsewhere.<sup>19</sup> Cleaning procedures were also reproduced in the Scienta ESCA 300 spectrometer at the Daresbury laboratory, again as described elsewhere.<sup>22</sup> Argon-ion bombardment was deliberately avoided as this causes preferential sputtering of oxygen and in  $\text{TiO}_2$  itself gives rise to strong band-gap emission.<sup>23</sup> It was found that annealing pellets in UHV at temperatures around  $620^\circ\text{C}$  led to surfaces with low levels of surface C contamination. The C  $1s$  to O  $1s$  intensity ratio was typically of the order of 0.08 for as-presented samples but was reduced by over a factor of 10 by

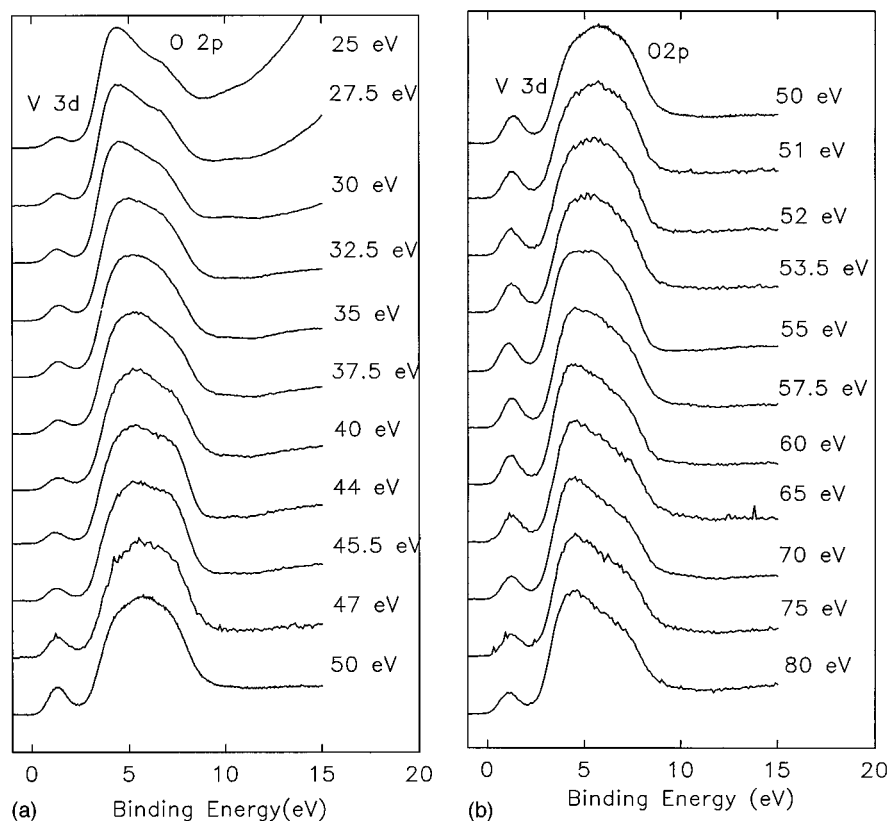


FIG. 2. Valence region photoemission spectra of 1% V-doped TiO<sub>2</sub> taken on beamline 6.2 at the different photon energies indicated. Binding energies are given relative to the Fermi energy of the sample mounting plate, which was determined by shifting the edge of the plate into the synchrotron beam. Spectra are normalized such that the O 2*p* maximum peak height is constant.

the *in situ* annealing. The reduced intensity ratio corresponds to a surface coverage by hydrocarbon contamination of less than 20% of a monolayer. Photoemission spectra of surfaces cleaned in this way were essentially free of structure to the high-binding-energy side of the O 2*p* valence band associated with unwanted adsorbates. Further reduction of the C 1*s* XPS intensity was possible by annealing at yet higher temperatures but always at the expense of segregation of trace K impurities present at the part per 10<sup>6</sup> level in the TiO<sub>2</sub>. These impurities were found to produce a marked attenuation of the V 3*d* band-gap intensity, probably due to formation of surface phases such as KVO<sub>3</sub>, which are more difficult to reduce than V-doped TiO<sub>2</sub>. The cleaning procedure eventually adopted on beamline 6.2 therefore involved annealing in UHV (base pressure 10<sup>-10</sup> mbar) at 620 °C for 2 h. This yielded a surface free of shallow core peaks due to K contamination and with a well-defined peak in the the TiO<sub>2</sub> band gap. There were no adsorbate-related peaks on the high-binding-energy side of the O 2*p* valence band.

### III. RESULTS AND DISCUSSION

X-ray photoemission spectra measured in the Daresbury Scienta spectrometer for as-presented samples with a nominal 1% vanadium doping level showed a pronounced V 2*p* doublet with an intensity corresponding to occupation of 18% of cation sites by vanadium [Fig. 1(a)]. This indicates that there is pronounced segregation of the V dopant to the polycrystalline V-doped TiO<sub>2</sub> surface. Annealing in UHV at

620 °C led to a decrease in the surface V concentration to around 11 cation % [Fig. 1(b)], along with broadening of the V 2*p* core-level peaks due to the emergence of a low-binding-energy shoulder. The V 2*p* intensity increased on going to grazing (10°) emission angle, indicating that the surface V distribution is not homogeneous on the depth scale relevant to XPS, with enhanced V concentration in the outermost ionic layers.

Photoemission spectra excited with synchrotron radiation over a range of photon energies between 25 and 80 eV are shown in Fig. 2. In each case the spectra contain a broad but well-defined O 2*p* valence band extending between 2.2- and 8.7-eV binding energy together with a weaker peak whose maximum intensity is at 1.3-eV binding energy.

The band gap of undoped TiO<sub>2</sub> is 3.0 eV (Ref. 30) and in very slightly oxygen deficient material the Fermi level is pinned by donor levels just below the bottom of the conduction band. The valence-band onset in UHV-annealed TiO<sub>2</sub> is therefore found at around 3.0 eV and the band-gap region has almost no photoemission intensity on nearly stoichiometric surfaces. These considerations establish that the peak at 1.3 eV occurs within the bulk band gap of the host TiO<sub>2</sub>. Pronounced oxygen deficiency in TiO<sub>2</sub> induced by ion or electron bombardment is signalled by the appearance of a peak at around 1-eV binding energy due to Ti 3*d* states which superficially looks very similar to the present band-gap peak. The 3*d* states in TiO<sub>2-x</sub> show resonant enhancement at the Ti 3*p* core threshold. The present photoemission energy distribution curves also show evidence of resonant

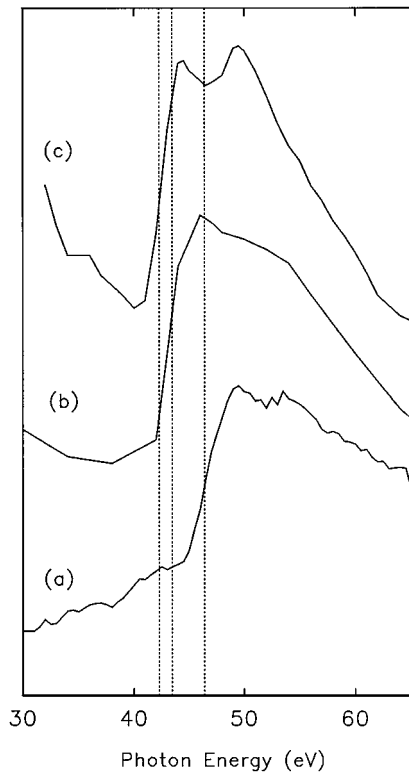


FIG. 3. CIS spectra (a) for band-gap states in V-doped  $\text{TiO}_2$  at 1.5-eV binding energy (present work). The count rate was normalized to the output from the tungsten mesh beam monitor and corrected for the quantum efficiency of the monitor. (b) For Ti  $3d$  states in ion-bombarded  $\text{TiO}_{2-x}$  taken from Ref. 24. (c) For Ti  $3d$  states in  $\text{TiO}_2$  (100)  $c(2 \times 2)$  K taken from Ref. 32. The midpoints of the resonance edges are indicated in (a)–(c), emphasizing the shift between (a) and the Ti  $3d$  data in (b) and (c).

behavior with a maximum intensity for the band-gap feature relative to the O  $2p$  valence band in the EDCs at 50.0 eV. This conclusion is confirmed by constant initial-state spectra. The CIS profile (Fig. 3) shows that the gap peak increases in absolute intensity by a factor of 4 on sweeping the photon energy between 30 and 50 eV. The maximum intensity is at 50.0 eV and the midpoint of the resonance “edge” is at 46.5 eV. For comparison, the corresponding resonance profile for  $\text{TiO}_{2-x}$  (Ref. 24) is also shown in Fig. 2. Here the midpoint of the resonance edge is at 43.5 eV, corresponding to a shift of 3.0 eV between the two data sets.<sup>31</sup> Figure 3 also shows a CIS profile from Ti  $3d$  states introduced into  $\text{TiO}_2$  by electron transfer from K deposited onto a (100) surface to give a  $c(2 \times 2)$  overlayer.<sup>32</sup> This resonance profile is similar to that for  $\text{TiO}_{2-x}$ , but with the midpoint of the resonance edge at the somewhat lower energy of 42.4 eV.

The resonance photoemission profiles establish that the gap peak is not associated with Ti  $3d$  states. This conclusion is supported by the observation that polycrystalline  $\text{TiO}_2$  surfaces subject to thermal annealing in UHV under conditions similar to those described here remain very nearly stoichiometric with an intensity of band-gap emission at least a factor of 20 weaker than found in the present work.<sup>33</sup> Moreover, the present resonance maximum is at the same energy as in  $\text{VO}_2$ .<sup>34</sup> In addition the shift of about 3 to 4 eV between Ti  $3d$  and V  $3d$  resonance profiles evident in Fig. 3 is es-

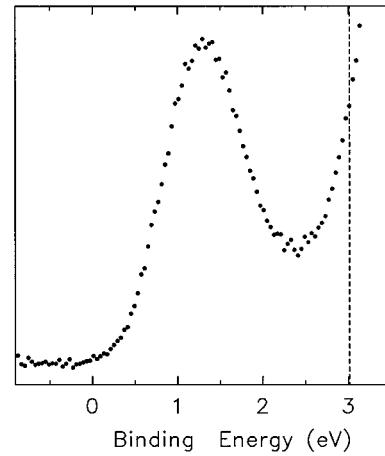


FIG. 4. Expanded scan of band-gap peak in 1% V-doped  $\text{TiO}_2$  excited at a photon energy of 50 eV. The dashed line indicates the position of the valence-band onset for  $\text{TiO}_2$  itself, emphasizing the shift to low binding energy found for V-doped  $\text{TiO}_2$ .

entially the same as that found between  $3d$  states in  $\text{Ti}_2\text{O}_3$  and  $\text{V}_2\text{O}_3$ .<sup>26,27</sup> It follows that resonance photoemission confirms the intuitively favored assignment of the gap states to electrons trapped on V dopant cations. The shift in the resonance may be compared with a somewhat larger shift of 5.7 eV between Ti  $3p$  and V  $3p$  core binding energies revealed by high-resolution XPS. This difference may be understood in terms of the localized nature of the excited state involved in the resonant photoemission process, whose energy is influenced both by the energy of the  $3p$  core level and the  $3d$  level to which the  $3p$  electron is excited.

It remains to consider the energy of the V  $3d$  state. Figure 4 shows an expanded scan of the band-gap peak and the O  $2p$  valence-band edge. The valence-band onset has shifted down by about 0.8 eV relative to the value of 3.0 eV found for undoped  $\text{TiO}_2$ . This demonstrates that the V(IV) dopant species have pinned the Fermi level about 0.8 eV down in the band gap. However, the peak maximum in the photoemission spectrum does not coincide with the Fermi level. This is because the Fermi energy is defined by the adiabatic ionization energy of the V  $3d$  states. In photoemission, the positions of ions surrounding the ionized V  $3d$  center are unable to relax on the time scale of the photoemission process. There is therefore a shift between the vertical and adiabatic energies of the V  $3d$  state corresponding to the energy associated with relaxation of ions around the ionized V  $3d$  center. This energy can be crudely estimated as  $E_R$  where

$$E_R = (e^2/8\pi\epsilon_0 r)[1/\epsilon(\infty) - 1/\epsilon(0)], \quad (1)$$

where  $r$  is the effective radius of the ionized state and  $\epsilon(\infty)$  and  $\epsilon(0)$  are the high- and low-frequency dielectric constants of the host lattice. More recently Fujimori and co-workers<sup>35</sup> have suggested a refinement of this approach applicable to self-trapped polaronic electrons by taking explicit account of relaxation of oxygen ions around the ionized center via an effective local force constant, together with longer-range polarization treated using Eq. (1) and a kinetic energy term associated with confinement of the electron. This approach

leads to a means of estimating the size of the polaron which minimizes the energy. However, in the present context the dopant electron is trapped by the impurity potential associated with the V dopant and we can roughly equate the effective size of the photohole with the ionic radius of V<sup>4+</sup> where  $r = 0.7 \text{ \AA}$ . Taking averages of the values for dielectric constants in tetragonal TiO<sub>2</sub> we thus estimate through Eq. (1) a

relaxation energy of 1.3 eV, in very pleasing agreement with the experimental value.

In summary, resonant photoemission has allowed identification of the atomic nature of band-gap states in V-doped TiO<sub>2</sub>. The technique should be of general value in probing the electronic structure of doped oxides and of locating electronic states associated with dopant atoms.

\* Author to whom correspondence should be addressed. Electronic address: Egdell@ermine.ox.ac.uk

- <sup>1</sup>B. O. Marinder and A. Magneli, *Acta Chem. Scand* **12**, 1345 (1958).
- <sup>2</sup>R. Kozłowski, R. F. Pettifer, and J. M. Thomas, *J. Phys. Chem.* **87**, 5176 (1983).
- <sup>3</sup>J. Ph. Nogier, J. Thoret, N. Jammul, and J. Fraissard, *Appl. Surf. Sci.* **47**, 287 (1991).
- <sup>4</sup>P. Lostak, Z. Cernosek, E. Cernoskova, L. Benes, J. Kroutil, and V. Rambousek, *J. Mater. Sci.* **28**, 1189 (1991).
- <sup>5</sup>P. Pomonis and J. C. Vickerman, *J. Catal.* **90**, 305 (1984).
- <sup>6</sup>F. Cavani, G. Centi, E. Foresti, F. Trifiro, and G. Busca, *J. Chem. Soc. Faraday Trans. 1* **84**, 237 (1988).
- <sup>7</sup>G. C. Bond, S. Flamerz, and R. Shukri, *Faraday Discuss. Chem. Soc.* **87**, 65 (1989).
- <sup>8</sup>G. Centi, D. Pinelli, F. Trifiro, D. Ghoussoub, M. Guelton, and L. Gengembre, *J. Catal.* **130**, 238 (1991).
- <sup>9</sup>A. Phillips, in *The Modern Chemicals Industry*, edited by H. Thompson (The Chemical Society, London, 1977).
- <sup>10</sup>D. Morris, B. A. Part II thesis, Oxford, 1996.
- <sup>11</sup>G. C. Bond, A. J. Sarkany, and G. D. Parfitt, *J. Catal.* **57**, 476 (1979).
- <sup>12</sup>A. Vejux and P. Courtine, *J. Solid State Chem.* **23**, 93 (1978).
- <sup>13</sup>J. F. Baumard and E. Tani, *J. Phys. Chem.* **67**, 857 (1977).
- <sup>14</sup>E. Tani and J. F. Baumard, *J. Solid State Chem.* **32**, 105 (1980).
- <sup>15</sup>F. Kubic and Z. Sroubek, *J. Chem. Phys.* **57**, 1660 (1972).
- <sup>16</sup>R. Gallay, J. J. van der Klink, and J. Moser, *Phys. Rev. B* **34**, 3060 (1986).
- <sup>17</sup>G. Chingas and L. Rowan, *Phys. Rev. B* **27**, 2636 (1983).
- <sup>18</sup>A. E. Taverner, Ph.D. thesis, Oxford, 1995.
- <sup>19</sup>A. E. Taverner, C. Rayden, S. Warren, A. Gulino, and R. G. Egdell, *Phys. Rev. B* **51**, 6833 (1995).
- <sup>20</sup>K. Mizushima, M. Tanaka, A. Asai, S. Iida, and J. B. Goodenough, *J. Phys. Chem. Solids* **40**, 1129 (1979).
- <sup>21</sup>K. Mizushima, M. Tanaka, and S. Iida, *J. Phys. Soc. Jpn.* **32**, 1519 (1972).
- <sup>22</sup>R. Dixon, R. G. Egdell, and G. Beamson, *J. Chem. Soc. Faraday Trans.* **91**, 3495 (1995).
- <sup>23</sup>V. E. Henrich and P. A. Cox, *The Surface Science of Metal Oxides* (Cambridge University Press, Cambridge, England, 1994).
- <sup>24</sup>Z. Zhang, S. P. Jeng, and V. E. Henrich, *Phys. Rev. B* **43**, 12 004 (1990).
- <sup>25</sup>S. Kodaira, Y. Sakisaka, T. Maruyama, Y. Haruyama, Y. Aiura, and H. Kato, *Solid State Commun.* **89**, 9 (1994).
- <sup>26</sup>K. E. Smith and V. E. Henrich, *Solid State Commun.* **68**, 29 (1988).
- <sup>27</sup>K. E. Smith and V. E. Henrich, *Phys. Rev. B* **38**, 9571 (1988).
- <sup>28</sup>D. Teehan (private communication).
- <sup>29</sup>R. H. Day, P. Lee, E. B. Saloman, and D. J. Nagel, *J. Appl. Phys.* **52**, 6965 (1981).
- <sup>30</sup>*Semiconductors. Physics of Non-Tetrahedrally Bonded Binary Compounds III*, edited by O. Madelung, Landolt-Börnstein, New Series, Group III, Vol. 17, Pt. g (Springer-Verlag, Berlin, 1984).
- <sup>31</sup>In making the comparison with these earlier data we are aware that the measurements were carried out on ion-bombarded TiO<sub>2</sub> using a cylindrical mirror analyzer whereas our own experiments employed an angle-resolving analyzer. As shown in Ref. 27, CIS profiles may be influenced by the acceptance characteristics of the analyzer when dealing with well-ordered single-crystal samples. However, the comparison shown in Fig. 3 relates to the polycrystalline ceramic sample of the present study and a disordered bombarded surface of the earlier work. Due to the nature of the samples we are basically dealing with angle-integrated spectra in each case.
- <sup>32</sup>K. Prabhakaran, D. Purdie, R. Casanova, C. A. Muryn, P. Hardman, P. L. Wincott, and G. Thornton, *Phys. Rev. B* **45**, 6969 (1992). The data in this publication were taken from the same beamline and with the same analyzer as in the present study.
- <sup>33</sup>A. Gulino, A. E. Taverner, S. Warren, P. Harris, and R. G. Egdell, *Surf. Sci.* **315**, 351 (1994).
- <sup>34</sup>S. Shin, S. Suga, M. Taniguchi, M. Fujisawa, H. Kanzaki, A. Fujimori, H. Daimon, Y. Ueda, K. Kosuge, and S. Kachi, *Phys. Rev. B* **41**, 4993 (1990).
- <sup>35</sup>A. Fujimori, A. E. Bocquet, K. Morikawa, K. Kobayashi, T. Saitoh, Y. Tokura, I. Hase, and M. Onada, *J. Phys. Chem. Solids*, **57**, 1379 (1996).